INTERNATIONAL JOURNAL OF MARITIME TECHNOLOGY
IJMT Vol.15/ Winter 2021 (131-146)

Introduction to a New Simple Spectral EWRUC Method for the Beach Cusps Formation (Case Study; Makoran Coast)

Elham Zakeri Anarak[1], Mehdi Adjami [2*], Amir Jabari Khameneh[3], Ahmad Rezaee Mazyak[4]

[1]*MSc. of Coastal Engineering, Shahrood University of Technology, elham.zakeri.a@gmail.com*
[2]*Assistant Professor of Coasts, Ports and Marine structures, Civil Engineering Department, Shahrood University of Technology, adjami@shahroodut.ac.ir*
[3]*Ph.D. Candidate of Coastal Engineering, Shahrood University of Technology, amir.jabarikh@shahroodut.ac.ir*
[4]*Ph.D. of Coastal Engineering, Tarbiat Modares University, a.rezaeemazyak@modares.ac.ir*

ARTICLE INFO

Article History:
Received: 29 Jun. 2021
Accepted: 15 Nov. 2021

Keywords:
Beach Cusps
Edge Wave Theory
Self-Organization Theory Mike 21 BW Module Makoran Coasts

ABSTRACT

Beach cusps are shoreline formations made up of various grades of sediment in an arc pattern. Many works are carried out to determine forming theories and effective parameters on cusps, and the standing edge wave and the self-organization theories are more acceptable. This study aims to investigate theories affecting cusps of Roudic port, located on Makoran coasts of Iran. The DHI MIKE software is used for modeling and the Madsen laboratory model is applied for the numerical-model calibration. A new method as Edge Wave and Run-up Comparison (EWRUC) is introduced, working by extracting the edge wave from energy density spectrum and comparing with run up, subsequently. This is a fast and simple (one dimensional) method for determining theory of cusp formation. Many scenarios adapted to the Roudic coast waves are based on monsoon and ocean waves. The results from EWRUC indicate that the theories of edge wave and self-organization are dominant in seasons of ocean-waves and monsoon-waves, respectively. EWRUC responses correctly to beaches that are similar to Roudic beach.

1. Introduction

Beach cusps are morphological phenomena on the beach surface that have 1) Horns to the sea with steep slopes and coarse sediments and 2) Bay or Embayment to the dry beach with gentle slopes and fine-grained sediments. Beach cusps are formed in most cases with swash currents, and are seen consistently and regularly parallel to the shorelines [1]. Beach cusps can reshape the coastlines in short time, but if the depth and the height of their embayment increases, it will erode the coastline, and if the sedimentation increases in its horn to the sea, it will lead to sedimentary miss effects for the structures nearby. Therefore, knowledge of the status and behavior of cusps' formation and development can be used to plan for future engineering projects and to adopt appropriate methods to deal with the unwanted effects of coastal changes and improve coastal management and its planning. The schematic and natural shape of beach cusps is shown in Fig. 1.

A wide range of theories has been proposed for the formation, configuration and preservation of natural beach cusps. In fact, any idea of cusps which has been presented in any research, violated in other ones. For example, for the effects of sedimentation and erosion have been said that cusps are the remaining features of erosion process [2, 3] or the emerging properties of the sedimentation process [4-7] otherwise they are effects of erosion and sedimentation processes [8-12]. In the case of distance between cusps, it is said that they have regular [13] or irregular intervals [2] .About the role of their morphodynamics, it is said that the water flow is related to the morphology of the cusp by the way water flows from the horn to the embayment [14,15] or from the embayment to the cusp's horn [16, 17] and the existence of large cusps is related to the formation of sand dunes [18-20]. In the cusps, there is a difference in the soil texture between the horn and the embayment [13, 17] or there is not [14, 21] .In the case of waves and tidal conditions, cusps evolve in high energy waves [11, 20, 22, 23] or form better in calm condition [24]. And the cusps are developed by incoming parallel wave [25], as well as the growth of the cusps is related to the normal incoming wave breaking angle [10, 22 and 26] or associated with the incoming diagonal wave [2, 21]. Morphodynamics feedback is more prominent than hydrodynamic forces [11] or hydrodynamics plays a more important role [27] and tides are effective on the formation of cusps [5, 7, 10, 18]. These ideas are said to have been fixed or violated, but despite a clear set of contradictory views, it seems that many confusions in studies are largely due to the descriptive and qualitative nature of these studies and researches. There are different viewpoints in mechanisms leading to the production of cusps. But in general, two theories have been accepted to describe the formation and behavior

[Downloaded from ijmt.ir on 2026-02-16]

of beach cusps, which are the standing edge wave [28] and self-organization theories [29, 30].

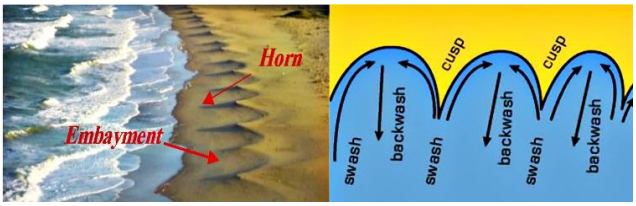

Figure 1. beach cusps

The main basis for studies is the review of the performance of two accepted theories for the formation of beach cusps .In general, the parameters involved in the formation of the beach cusps are beach slope, wave run up and type and characteristics of the region's waves and the parameters affecting the size and intervals of the cusps, according to the standing edge wave theory the parameters involved in the formation of the cusps are the wave period and the beach slope and according to the theory of self-organization is the length of the swash [31].

This study aimed to investigate the theory that effects the cusps and a valid experimental model has been used for model calibration. After that, modeling of Roudic beach is carried out and 18 scenarios according to the waves dominating the Roudic coasts adapted. Finally, a new method called EWRUC is presented that has not been proposed and used before. In this method, the The first relation is for sub-harmonic edge wave (twice the wave period of the incoming wave) and the second relation is for the synchronous edge wave (the incoming wave period is equal to the edge wave period) [30].

Self-Organization Theory: this theory has two main points; positive feedback between coastal morphology and swash flow creates ups and downs patterns (topographic irregularities) on the coast. Areas with lower patterns cause the particles to fall, and increase the velocity and energy of the particles, and this water energy will erode the surface of the beach, causing the embayment in the cusps. Negative feedback reduces the amount of erosion and sedimentation. When the wave hits the horn, it will lose energy and sediments will settle. The loss of these sediments gives rise to the energy of water, which results in the removal of sediments from the cusps embayment in the returning wave. The results of the self-organization model predict that:

$$\lambda_c = f \cdot S_e \qquad (3)$$

In which λ_c is the cusp spacing, S_e represents the swash excursion length (the horizontal distance between the most progressive and reversible swash current at the coast or the vertical distance between the edge wave that derived from the energy density spectrum is compared with run up, and it is determined that the formation of cusps follows the edge wave theory or not. The analyzed results of Roudic models and the analysis of EWRUC method were identical, which show that this method is reliable.

2. Theories of Cusps Formation

Edge Wave Theory: edge waves are low-frequency periodic waves, propagating parallel to the beach and trapped near the beach due to refraction. When the two edge waves come from two opposite directions, a standing edge wave form. When a standing edge wave conforms to an incoming wave, systematic alongshore variation in the coastal system is made in the height of swash, and a regular erosion disorder results in the formation of a cuspate pattern. Relationships 1 and 2 are presented for the intervals of the cusps. In these relations, λ_c is the distances between the cusps, T is the incoming wave period, $\tan\beta$ is the coast gradient and g are the acceleration of gravity.

$$\lambda_c = \frac{g}{\pi} T^2 \tan\beta \qquad (1)$$

$$\lambda_c = \frac{g}{2\pi} T^2 \tan\beta \qquad (2)$$

run up and the run down) and f denotes as a geometric parameter in the range of 1 to 3 [8, 32].

In the course of some of studies, a strong connection is found between cusp spacing and the swash excursion length, which supports the self-organization theory. It is also found that the formation of cusps has a better correlation with the theory of self-organization [6, 7, 9, 14, 16, 25, 33, 34].

On the other hand, other studies have shown that the distances and formation of the cusps are related to the edge wave theory [1, 8, 15, 27, 35], but other studies have shown that both theories in the formation and distance between the cusps are acceptable [3, 10, 33].

3. Study Area

Roudic port with 25.19° latitude and 61.08° longitudinal coordinates in Sistan and Baluchistan province of Iran and in coastal areas of Chabahar city (Makoran coasts) is located at 40 km from the Chabahar port; the ports of Beris and Ramin are the nearest ports to it. Figure 2 shows the position of the Roudic port on the southern coasts of Iran at Oman sea.

The beaches of the Roudic area due to the formation of beach cusps are a very good place to identify and simulation of cusps, including comparison with laboratory models, and numerical control and modeling. The beaches under study are within the boundaries of the Roudic area in the range of monsoon

[Downloaded from ijmt.ir on 2026-02-16]

beaches. The features of these beaches include monsoon waves with a height of less than 3 meters, 3 to 4 meters for depth of water near the coast, beach surface with well-sorted medium sand, gentle bed slope, sedimentation in ports and closure of the spouts of rivers are according to the seasonal pattern of waves and precipitation conditions [36].

Figure 2. Location of the Roudic Port on the shores of the Oman Sea (Google Earth)

3-1. Roudic Coast Data

The studies of coastal modeling in the province of Sistan and Baluchistan were defined by Ports & Maritime Organization of IRAN (IRANIAN PMO) for a period of 23 years (1985-2007) conducted with cooperation of JWERC and the Baird Canadian company within the coastal zone of Sistan and Baluchistan in the Oman Sea. The wave rose shown in Fig. 3 is plotted according to the direction and height of the available waves. The dominant direction of the wave is 200 degrees, which is characterized by the perpendicularity of the wave rose to the Roudic coast, and $D_{50} = 0.30mm$ is the average size of the bed sediment particles [37]. There are two types of dominant waves in the area during a year, which are oceanic and monsoon waves, respectively. Monsoon waves form by the inflow of air on the subcontinent of India with a height of 0.3 to 1.5 meters and period of about 10 to 13 seconds. Oceanic waves began from the South Pole and in the direction of the Indian Ocean, reaching the Makoran coastline, have found high wave's characteristics with long wavelengths and long periods. The wave height of these waves has changed from 0.25 to 1.00 meter and their period varies from 16 to 18 seconds. The surveys show that the Roudic beach is a subset of the wave dominate coasts, and this area is among the high wave energy shores [31]. Section 5.1 of this study describes the monsoon and oceanic waves, and also the numerical modeling scenarios are expressed. Also, Field observations have been made and available data suggest that the slope of the Roudic beach during the year has not changed much and the slope can be considered practically constant.

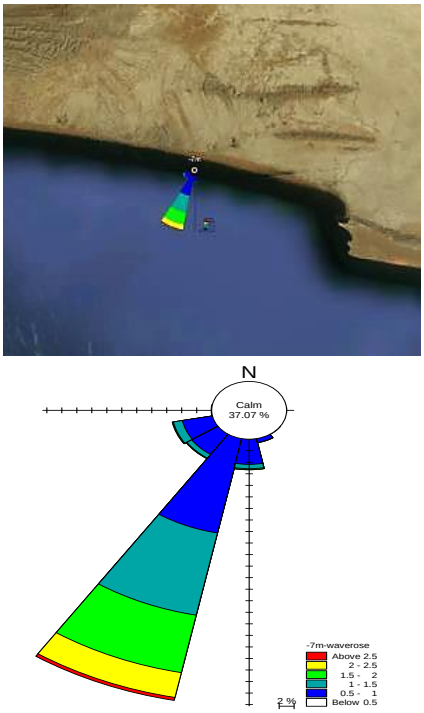

Figure 3. The wave rose of Roudic area [37]

4. Numerical Modeling

To examine and predict the factors affecting the large-scale sea-based patterns, it is possible to use the long-term field studies with a great deal of cost or use of powerful software for modeling. In this research, the DHI MIKE software, one of the most powerful software in the field of maritime hydrodynamic and morphological issues, was used.

4-1. Model (DHI Mike)

The module used in this software is MIKE21-BW because it has the ability to model the effects of waves on the swash area. The 1DH Boussinesq wave module used in this study although two-dimensional modeling for the swash zone offers the best results but the use of one-dimensional models and its estimates for swash zone identification has been used in many studies [39, 41]. The application of the BW 1D model is in researchs conducted in the Swash zone and the use of real information for modeling, not considering future predictions and check existing status are its positive points [38]. Similar to published article by Madsen et al in 1997 a simplification is used to eliminate the two-dimensional problem and turn it into one dimension, which is the slot technique.

The 1DH Boussinesq wave module has classical and advanced Boussinesq equations. Classic Boussinesq equations are used when the ratio of the maximum depth of water to the wavelength in deep water (h_{max}/L_0) is less than 0.22, and advanced Boussinesq equations, which include deep water components, allow the model to develop under deeper water conditions and a smaller wave period, such as $0.5 = h_{max}/ L_0$. The one-dimensional module needs to consider the deep-water components that due to the

[Downloaded from ijmt.ir on 2026-02-16]

region's wave conditions, deeper water conditions are used in the model. One of the important issues when solving Boussinesq's equations with the use of the finite element technique is the presence of higher-order spatial derivatives. This problem is controlled here by using a method in which Boussinesq equations are controlled by introducing a new auxiliary variable (w) and an auxiliary algebraic equation in lower order. The governing equations have the following form [38].

$$n\frac{\partial \xi}{\partial t}+\frac{\partial P}{\partial x}=0 \qquad (4)$$

$$w=\frac{\partial}{\partial x}(d\frac{\partial \xi}{\partial x}) \qquad (5)$$

$$n\frac{\partial P}{\partial t}+\frac{\partial}{\partial x}\left(\frac{P^2}{h}\right)+\frac{\partial R_{xx}}{\partial x}+n^2gh\frac{\partial \xi}{\partial x}-$$
$$n(B+\frac{1}{3})d^2\frac{\partial^3 P}{\partial x\,\partial x\,\partial t}-\frac{1}{3}d\frac{\partial d}{\partial x}\frac{\partial^2 P}{\partial x\,\partial t} \qquad (6)$$
$$-n^2Bgd^2\frac{\partial w}{\partial x}+$$
$$n^2P\left[\alpha+\beta\frac{|P|}{h}\right]+\frac{gP|P|}{h^2C^2}=0$$

In this equation R_{xx} is equal to:

$$R_{xx}=\frac{\delta}{1-\delta/d}(c_x-\frac{P}{d})^2 \qquad (7)$$

These parameters are: flux density in the x-direction p $(m^3/m/\sec)$, Boussinesq dispersion factor B, Cartesian coordinates system x (m), time t (sec), total depth of water d $(=h+\xi)$ (m), still water depth h (m), gravitational acceleration g $(9.81m/s^2)$, porosity coefficient n, Chezy resistance number C $(m^{0.5}/\sec)$, resistance coefficient for laminar flow in porous media α, resistance coefficient for turbulent flow in porous media β, water surface level above datum ξ (m), thickness of the surface roller δ and roller celerity component C_x. A number of parameters are shown in Fig. 4. The equations include wave breaking fracture effects based on the concept of surface rollers, which assumes that the effect of wave breaking can be modeled by applying a volume of water (rollers) in front of the wave (from the breaking point) and the wave velocity c. C_x and C_y are the roller celerity components or wave; δ is the roller thickness, which is equal to the height of the water from the level of water to the tangent of the wave gradient, u and v are the velocity distribution of the particles in the direction of x and y respectively [38, 39].

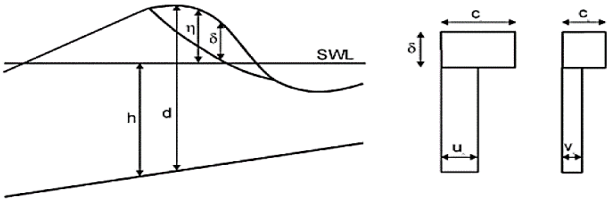

Figure 4. Sketch showing the principles of the surface roller concept. Left part shows a cross section of the breaking wave. Right side shows the assumed profile of horizontal particle velocity components. Figure from [39]

4-2. Calibration and Validation of the Numerical Model

Due to the lack of recorded data for changes in the coastline from wave breaking zone to Iran's coastline for the calibration of the numerical model, a published article by Madsen et al 1997, which is about nonlinear dynamic waves in the breaking zone has been used. This paper is also used to calibrate the BW MIKE module and is referenced in the software guide section.

Before validating the model; First, sensitivity analysis was performed on the model results by changing the parameters, and then by finding significant relationships between the effective parameters of the model validation was performed by comparing the results of Madsen's article [31, 39]. This paper uses the Mase laboratory direct flume data from 1994, with a Straight length of 10 meters, water depth of 0.47 meters and a length of 12 meters with a slope of 1/20, as shown in Fig. 5. For calibration, WG8 and WG10 wave makers information are used according to Madsen's paper, and the results are shown in a frequency of 1.0 Hz [39, 40].

For the numerical model, the sponge layer is used at the boundary of the incoming wave in the boundary of the coast to remove the instabilities due to the return of the waves to the model boundary and also as an ending point of the waves when they arrive at the coast. And the filter layer on the side of the coast avoids the instability of the numerical model by eliminating the high frequencies of model and preventing negative depth when the wave reaches the coast. The location of the sponge and filter layers is shown in Figure 6 (a and b).

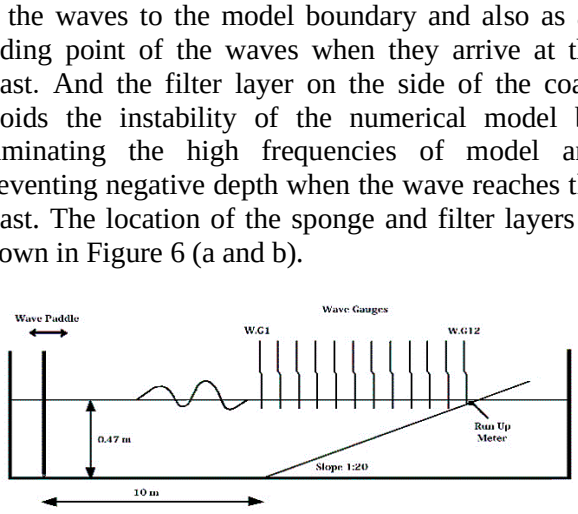

Figure 5. Sketch of physical wave flume [40]

[Downloaded from ijmt.ir on 2026-02-16]

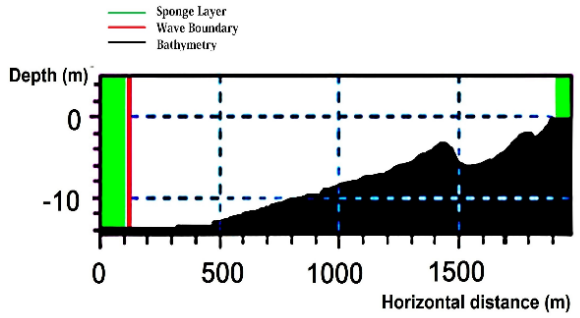

a. Sponge Layer

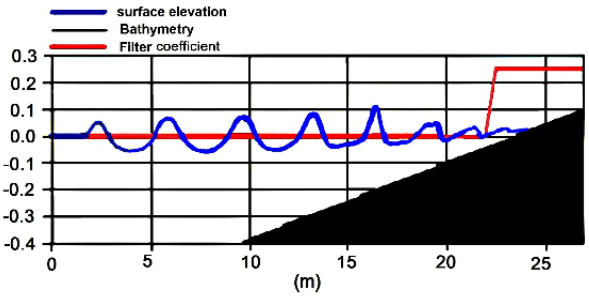

b. Filter Layer

Figure 6. Boundary condition and structure of the one-dimensional BW model [38]

4-3. Laboratory Modeling Scenarios

For accurate calibration, seven scenarios adapted in this study, the results of the calibration are given to the frequency of $f_m = 1HZ$ and distance of $\Delta = 5cm$ for the meshes. In Tables 1 and 2, for a better understanding of the changes, the preliminary guess has been used from Nielsen and Simonsen paper [41]. By examining the results of Tables 1 and 2 and the default parameters of numerical model (Case None), the need for changes in the calibration parameters was determined. Accordingly, Table 3 presents the proposed scenarios for the numerical model. In all scenarios, 1500-time steps are considered for the warm-up. It should be noted that in the calibration section, comparisons are performed qualitatively because the data of this laboratory test is not available, but the results are very close.

Table 1. Coastline scenarios [41]

Cases	Slot depth	Slot width	Slot smoothing	Slot friction
Case1	-0.3	0.001	100	**0**
Case2	-0.3	0.0019	100	**0**
Case3	-0.3	0.008	100	**0**
Case4	-0.3	0.005	100	**0.01**
Case5	-0.3	0.005	100	**0**
Case6	-0.3	0.01	100	**0**

Table 2. Scenarios of wave breaking parameter [41]

Cases	Roller form	Roller celerity	Initial breaking	Final breaking	Half-time cut-off roller
Case7 (t_3)	1.5	1.3	22°	10°	T/5=0.21
Case8 (t_1)	1.5	1.3	22°	10°	0.21
Case9 (t_3)	1.5	1.3	20°	20°	0.21
Case10 (t_1)	1.5	1.3	20°	20°	0.21

Table 3. Scenarios for the model Adapted

Cases	Slot depth	Slot width	Slot smoothing	Slot friction
Case1+1	-1.5	0.001	100	0
Case1+2	-1.5	0.1	100	0
Case1+3	**-2.10**	**0.001**	**100**	0
Case1+4	-2.10	0.001	100	0
Case1+5	-2.10	0.001	100	0

Cases	Roller form	Roller celerity	Initial breaking	Final breaking	Half-time cut-off roller
Case1+4 (t_1)	1.5	1.3	22°	10°	T/5=0.21
Case1+5 (t_3)	1.5	1.3	22°	10°	0.21

4-4. Calibration Results of BW Module

By comparing all of the scenarios, Case1+3 scenario shows the characteristics of the calibrated model. The results of surface elevation in WG8 and WG10 wave gauges, which have 338 and 358 codes, are compared with the results of Madsen's paper and are shown in Figures 7 and 8, parts A and B. It is seen that the elevation values at the depths have a minimum of -0.02 and -0.014 as well as at the peaks have a maximum of 0.029 and 0.030, which are very much close to each other in the laboratory model and test . By reducing values of the slot depth, the values of surface elevation decrease. Also, the slot width parameter influences the fuzzy changes of the results, which were reduced by the amount of 0.1 from the default values of the MIKE and the laboratory test and model results shown a very good collaboration. Considering the above issues, the MIKE one-dimensional BW model is calibrated.

Regarding the convergence of the numerical method, it is noted that the software calculates the Courant number according to the mesh intervals and the time interval. The Courant number in the one-dimensional model according to the MIKE software manual should be between 0 and 0.5, which for the Roudic model varies from 0.2 to 0.25 and is calculated by the software. It should be noted that in this section, comparisons have been made qualitatively because the data of this laboratory test are not available, but the results are still very close.

[Downloaded from ijmt.ir on 2026-02-16]

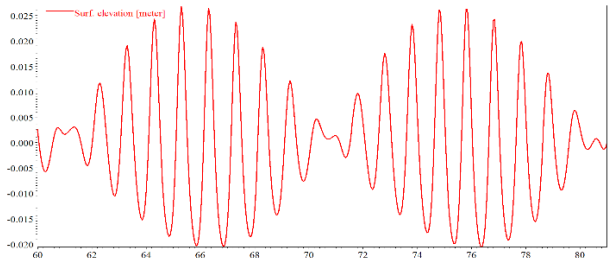

A. Output of surface elevation, modeling in code 338

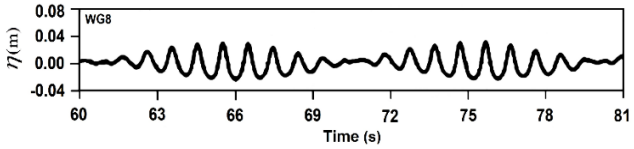

B. Surface elevation experimental data by Madsen [39]

Figure 7. A and B, comparison of outputs in WG8 wave-gages

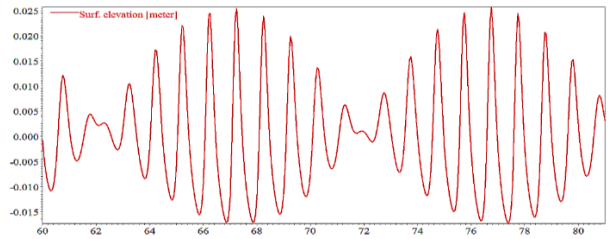

A. Output of surface elevation, modeling in code 358

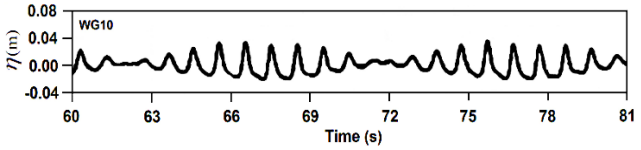

B. Surface elevation experimental data by Madsen [39]

Figure 8. A and B, comparison of outputs in WG10 wave-gages

5. Roudic Coasts Modelling, Analysis and Review

The components of the one-dimensional BW module are:

A. Bed Profile: the profile of the Roudic beach is 1700 meters long and the mesh distances are 0.50 meters. The depth profile changes are from -8.12 meters at the deep-water side and +2.68 meters on the side of the coast, as shown in Figures 9 and 10.

B. Surface Elevation due to the Incoming Wave of the Roudic Model: The Johnswap spectrum is considered due to H_{m0} and T_P for all modeling scenarios in Section 4-1, and the output of surface elevation is extracted. For example, the surface elevation for one of the scenarios are shown in Figure 11.

C. The Sponge layer: it is located in the boundary conditions of the incoming wave and in the swash zone, also it depends on the characteristics of the deep-water wavelength (L) and the profile of mesh distances (Δ). For example, a sponge layer of modeling scenarios is shown in Figure 12.

D. The Filter Layer: it is located in the swash zone and depends on mesh distances. According to Roudic modeling scenarios and uniform mesh dimensions, only one type of filter layer is used, as shown in Figure 13.

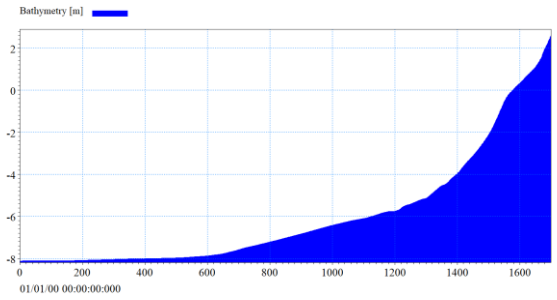

Figure 9. Roudic Beach profile in the BW-1D module

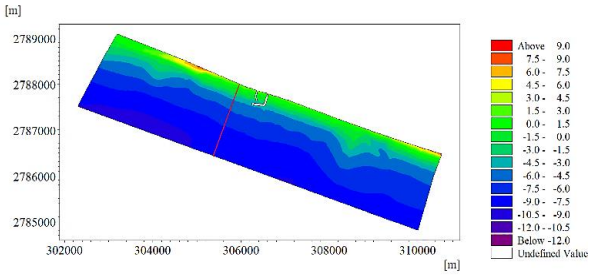

Figure 10. Two-dimensional hydrography of the port of Roudic and the location of the selected profile

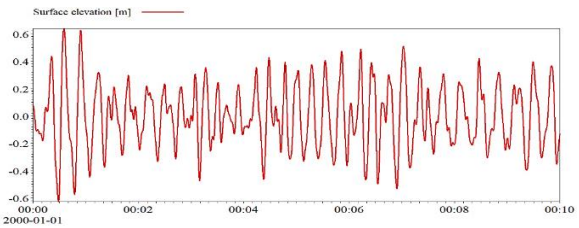

Figure 11. Incoming wave Surface elevation of the Roudic model in time unit, 9th scenario

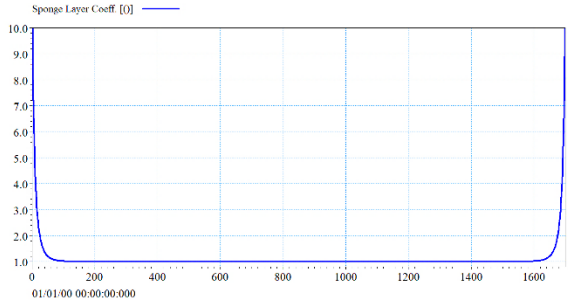

Figure 12. Roudic Beach sponge layer in BW-1D module

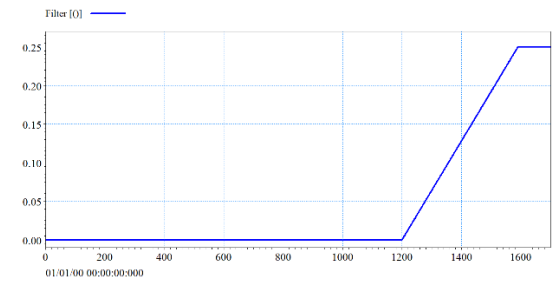

Figure 13. Roudic Beach Filter layer in the BW-1D Module

5-1. Oceanic Waves versus Monsoon Waves

[Downloaded from ijmt.ir on 2026-02-16]

The Makoran coast is a subset of monsoon beaches. In order for a better description of the regional waves, according to figure 14, the time series of the 22-year-old buoy wave data for Roudic is shown between 1985 and 2007.

As shown in figure 14 and the red circle, in mid-year of every year, the highest wave height is recorded, and this trend has been repeated throughout all the years. Figure 15 shows an example of the 2006 wave variation in detail, the blue lines are the Significant wave height and the red lines are the waves period, according to the explanation of section 3 and the introduction of the dominant waves of the Makoran coast from the middle of May to the middle of September, the waves heights are 1.50 to 3.0 meters, representing monsoon waves. The peak of the waves was in July, and the trend continued to decline until mid-September, when Monson's waves ended. The corresponding period is also in the range of 10 to 13 seconds. From early January to mid-May and from mid-September to the late December, the wave's height is 0 to 1.50 meters, and their corresponding period is 15 to 18 seconds, representing ocean waves. According to the characteristics of the waves in the Makoran coast, it can be said that the monsoon waves are about 5 months of a year and the ocean waves are about 7 months of a year. In order to construct the numerical model and the correct analysis, the scenarios should be based on these facts.

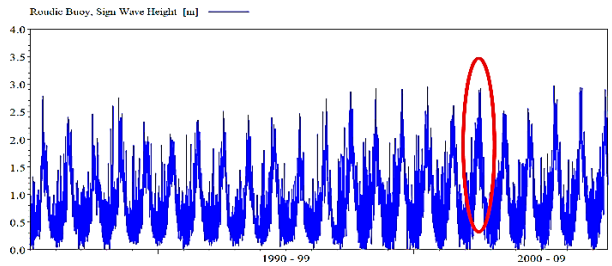

Figure 14. 22-year time series (1985 to 2007) waves in buoy of Roudic

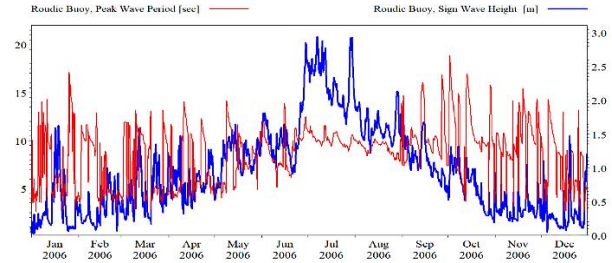

Figure 15. Time series of Roudic waves of buoy in 2006

5-2. Modeling Scenarios

Based on the regional waves and the explanations presented, 18 scenarios covering all modes for the implementation of the numerical model are presented in Table 4. These scenarios have been analyzed and the results are expressed in the following.

Table 4. Modeling Scenarios

Waves	Scenarios	H_{m0} (m)	Wave Type	T_p (Sec)
Oceanic Waves	*1*	0.50	*Jonswap Spectrum*	*16*
	2	0.50	*Jonswap Spectrum*	*17*
	3	0.50	*Jonswap Spectrum*	*18*
	4	0.75	*Jonswap Spectrum*	*16*
	5	0.75	*Jonswap Spectrum*	*17*
	6	0.75	*Jonswap Spectrum*	*18*
	7	1.00	*Jonswap Spectrum*	*16*
	8	1.00	*Jonswap Spectrum*	*17*
	9	1.00	*Jonswap Spectrum*	*18*
Monsoon Waves	*10*	1.50	*Jonswap Spectrum*	*11*
	11	1.50	*Jonswap Spectrum*	*12*
	12	1.50	*Jonswap Spectrum*	*13*
	13	2.00	*Jonswap Spectrum*	*11*
	14	2.00	*Jonswap Spectrum*	*12*
	15	2.00	*Jonswap Spectrum*	*13*
	16	2.50	*Jonswap Spectrum*	*11*
	17	2.50	*Jonswap Spectrum*	*12*
	18	2.50	*Jonswap Spectrum*	*13*

According to Table 5, with increasing in the wave's period and height, swash length and cusps penetration length increase; increasing in length leads to the formation of cusps with larger penetration and larger size. The cusp spacing parameter is increased by increasing the wave period due to edge wave theory and are closer to reality in comparison with the values of the self-organization theory, so the effect of the edge wave theory on formation of cusps with these types of waves is observed.

According to Table 6, by increasing period and height of the wave, swash length and cusps penetration length increase, which is obvious due to the run-up length of the wave, leading to the formation of larger penetration and larger sizes for cusps. The cusp spacing parameter using the theory of self-organization is closer to reality than the values obtained from the edge wave theory, so the effect of the theory of self-organization on the formation of cusps with these types of waves is observed. The spacing between cusps, while using self-organization theory increases due to increasing the wave height and thus increasing the length of the swash.

By comparing the two scenarios, the oceanic and monsoon waves, it is observed that in ocean waves, as the wavelength rises from 0.5 to 1.00 meters, the resulting run up increases. However, along with the height of the waves, the period also plays an important role in the increasing of the wave run up, which increases with increasing the period from 16 to 18 seconds. Also, in monsoon waves, due to the increase in the height of the waves from 1.50 to 2.50 meters, the run up has increased, as well as an increase in the period of waves from 11 to 13 seconds. Considering that the run up of ocean waves due to table 5, is 5.90 to 11.50 meters, and run up of monsoon waves

[Downloaded from ijmt.ir on 2026-02-16]

according to table 6, is in change from 18.80 to 35.30 meters. It is obvious that due to the higher run up in the monsoon, the cusps formed in the Oceanic scenarios are located at the lowest point of the swash zone up to the sea and in the Monsoon, scenarios are located upper than that. It can be said that their behavior is in line with the red and blue lines in Figure 16.

Measured cusps spacing at the time of the Monson were about 18 to 28 meters and the cusps spacing during the ocean waves were 7 to 13 meters, which, as mentioned before, was consistent with the numbers obtained through modeling.

Table 5. Cusp's characteristic of the ocean waves scenarios

SC	*Bed Slope*	H_s *(m)*	Type of Wave	T*(sec)*	Run up *(m)*	Run Down *(m)*	As *(m)*	Cusps (Max Penetration)	λ_{ew}	λ_{so}
1	*1:60*	*0.50*	*JONSWAP*	*16.00*	*5.90*	*-1.45*	*3.675*	*5.90*	*13.32*	*5.513*
2	*1:60*	*0.50*	*JONSWAP*	*17.00*	*6.14*	*-1.49*	*3.815*	*6.14*	*15.04*	*5.723*
3	*1:60*	*0.50*	*JONSWAP*	*18.00*	*6.40*	*-1.52*	*3.960*	*6.40*	*16.86*	*5.940*
4	*1:60*	*0.75*	*JONSWAP*	*16.00*	*8.20*	*-1.75*	*4.975*	*8.20*	*13.32*	*7.463*
5	*1:60*	*0.75*	*JONSWAP*	*17.00*	*8.40*	*-1.79*	*5.095*	*8.40*	*15.04*	*7.643*
6	*1:60*	*0.75*	*JONSWAP*	*18.00*	*8.70*	*-1.70*	*5.200*	*8.70*	*16.86*	*7.800*
7	*1:60*	*1.00*	*JONSWAP*	*16.00*	*10.70*	*-1.87*	*6.285*	*10.70*	*13.32*	*9.428*
8	*1:60*	*1.00*	*JONSWAP*	*17.00*	*11.20*	*-1.90*	*6.550*	*11.20*	*15.04*	*9.825*
9	*1:60*	*1.00*	*JONSWAP*	*18.00*	*11.50*	*-1.95*	*6.725*	*11.50*	*16.86*	*10.088*

Table 6. Cusp's characteristic of the monsoon waves scenarios

SC	*Bed Slope*	H_s *(m)*	Type of Wave	T*(sec)*	Run up *(m)*	Run Down *(m)*	As *(m)*	Cusps *(Max Penetration)*	λ_{ew}	λ_{so}
10	*1:60*	*1.50*	*JONSWAP*	*11.00*	*18.80*	*-6.00*	*12.400*	*18.80*	*6.297*	*18.600*
11	*1:60*	*1.50*	*JONSWAP*	*12.00*	*20.50*	*-6.90*	*13.700*	*20.50*	*7.495*	*20.550*
12	*1:60*	*1.50*	*JONSWAP*	*13.00*	*22.00*	*-7.10*	*14.550*	*22.00*	*8.796*	*21.825*
13	*1:60*	*2.00*	*JONSWAP*	*11.00*	*24.30*	*-8.90*	*16.600*	*24.30*	*6.297*	*24.900*
14	*1:60*	*2.00*	*JONSWAP*	*12.00*	*26.60*	*-8.80*	*17.700*	*26.60*	*7.495*	*26.550*
15	*1:60*	*2.00*	*JONSWAP*	*13.00*	*28.00*	*-8.70*	*18.350*	*28.00*	*8.796*	*27.525*
16	*1:60*	*2.50*	*JONSWAP*	*11.00*	*32.00*	*-10.00*	*21.000*	*32.00*	*6.297*	*31.500*
17	*1:60*	*2.50*	*JONSWAP*	*12.00*	*33.30*	*-9.20*	*21.250*	*33.30*	*7.495*	*31.875*
18	*1:60*	*2.50*	*JONSWAP*	*13.00*	*35.30*	*-8.30*	*21.800*	*35.30*	*8.796*	*32.700*

Figure16. Beach cusps at Roudic beach (Google Earth)

6. Introduction of a New Method for Detecting Cusps Formation

To find out how cusps form, a new method is introduced in this study, called Edge Wave and Run up Comparison method (EWRUC). The purpose is not to generalize this method to any coast with different conditions but the goal is to devise a method for conditions similar to those of the Roudic Beach. EWRUC depends on the formation of waves, the breaking of waves and eventually the run up of waves on the coast as well as it can be used in the same conditions as the Roudic beach. In the EWRUC method, a comparison is made between the amount of wave run up along the coast and the edge waves extracted from the numerical model.

[Downloaded from ijmt.ir on 2026-02-16]

To derive edge waves from a numerical model, firstly, the wave breaking zone must be identified, since the maximum energy of the waves is generated in the breaking zone and the edge waves are formed in this region. In order to identify the breaking zone, the linear changes of the bed profile and the significant wave height were drawn in Figures 17 and 18, the horizontal axis defines changes in cross-shore profile and the vertical axis of the left side defines changes in the depth profile and the right vertical axis denotes the significant wave height variations while all are measured in meters. Accordingly, as an example, the variations of significant wave height along the cross-shore profile of the bed are plotted for scenario 1 as ocean waves and the scenario of 10 as monsoon waves. Figure 17 shows that waves with a height of 1.51 meters began from the boundary of the model and decrease in height due to interactions with returned waves, and again experience a sudden increase in their height and reach to the height of 1.50 meters followed by a sharp decrease in wave's height and again reach to zero. The red arrow is the location of the breaking zone of the waves and its equivalent depth is the depth of the breaking zone, which is obtained 3.0 meters when is perpendicular to the bed profile. Figure 18 has the same status as figure 17. In that case, the depth of wave breaking is about 3.0 meters and of course by manual calculation this figure is obtained about 3.10 meters.

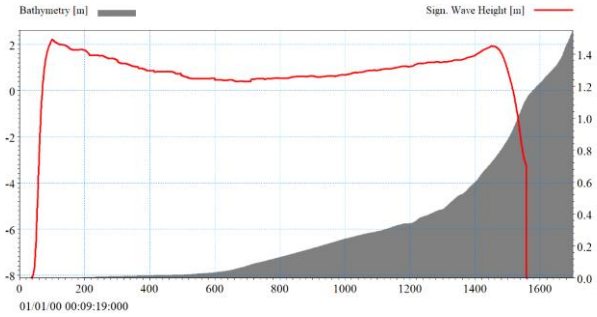

Figure 17. Significant wave height changes profile with the bed profile for determine the wave breaking area, 10th monsoon wave's scenario

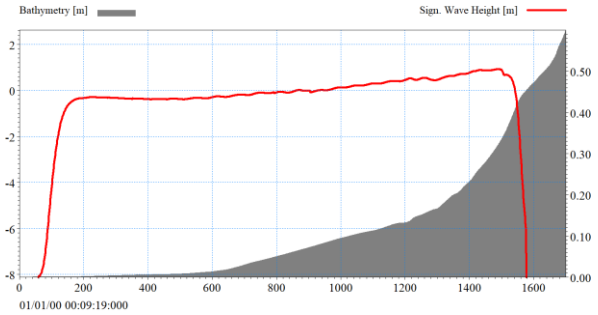

Figure 18. Significant wave height changes profile with the bed profile for determine the wave breaking area, 1st ocean wave's scenario

In this step, for extraction of the edge wave from the numerical model and performing accurate analysis on the creation location of these waves, the three areas of before, after and the breaking zone for the surface elevation are extracted and by using the fast Fourier transform (FFT) function, the energy density spectrum in all three points are extracted. As shown in Figures 19 and 20, the spectral density of wave's energy for scenarios 1 and 10 is extracted as an example. The horizontal axis of the graphs is the frequency (Hz unit) and the vertical axis is the energy density of the waves. Figure 19 shows that before the breaking zone, the energy of the waves is at a peak. After the breaking waves, the energy turns into two red and blue lines, and the edge waves have a period of between 15 and 25 seconds. According to the Figure 19, the orange zone shows the location of the formation of edge waves in the monsoon wave scenarios, but in Figure 20, the energy reduction is not as tangible as Figure 19 but the energy loss can be seen in the breaking process.

It also can be seen that the maximum energy form at the frequency of about 0.06 Hz or 17 seconds, which indicates the edge wave. Therefore, to determinant the location of the formation of the edge waves, the function of FFT performed on the surface elevation again, and by filtering in the desired frequency range, surface elevation of the edge waves obtained.

[Downloaded from ijmt.ir on 2026-02-16]

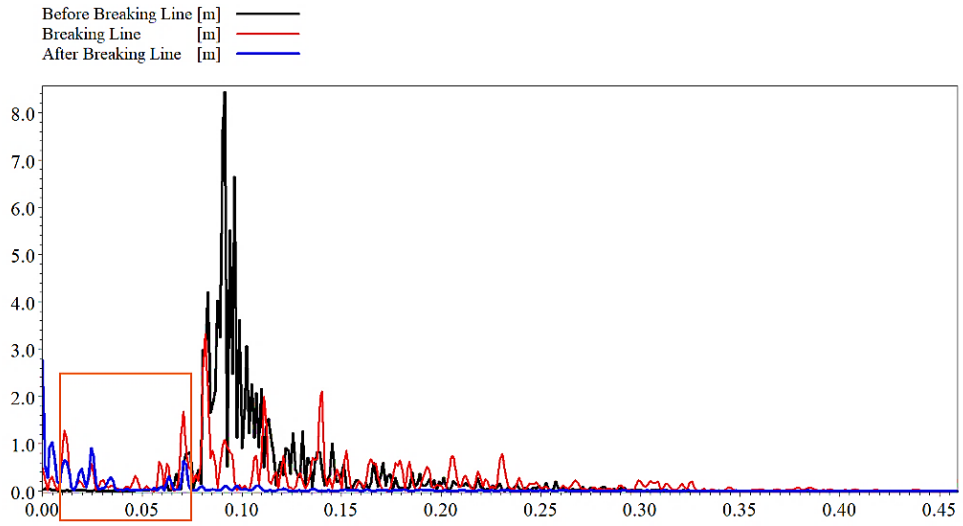

Figure 19. Energy density spectrum in three areas before, after and breaking zone, 10th scenario of monsoon waves

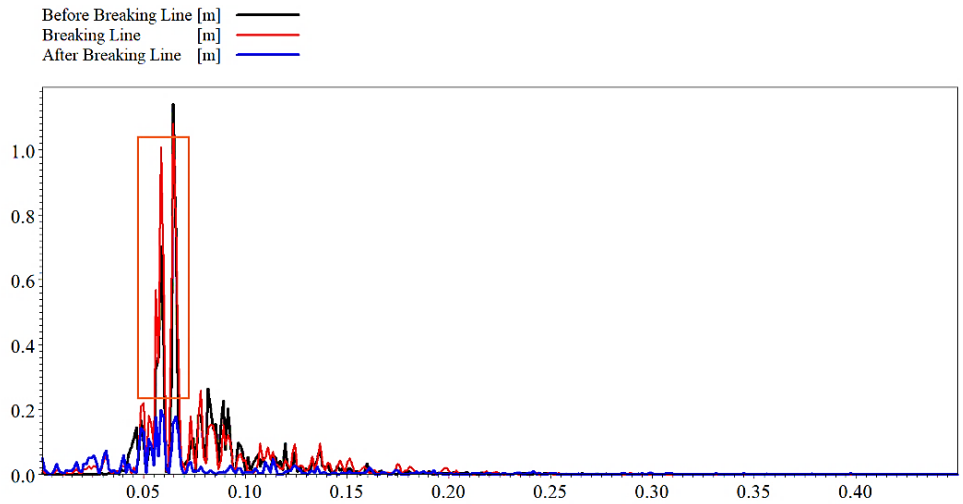

Figure 20. Energy density spectrum in three areas before, after and breaking zone, 10th scenario of ocean waves

[Downloaded from ijmt.ir on 2026-02-16]

Also, as an example, the output of surface elevation in scenario 10 is compared with the surface elevation caused by the edge waves of scenario 10 in Figure 21, in which the edge wave and the incoming waves are both fluctuating and approximately at the same phase.

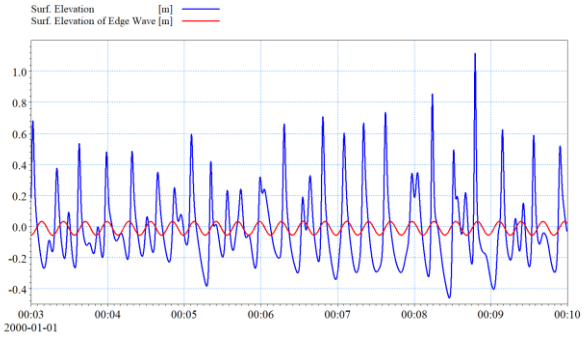

Figure 21. Display of the variation of edge waves and incoming surface elevations 10th scenario

In the end, by overlapping the outgoing edge wave and the total wave run up, the formation of coastal cusps determined. In Section 2, it was stated that the main factor in the formation of cusps using edge wave theory is the edge waves. Therefore, when edge waves and their total wave run up have the same oscillatory pattern or fluctuate; it can be said that cusps follow the edge wave theory, and if they have a reverse function or do not have a similar pattern, self-organization theory is dominant. This method has been used to investigate the Madsen laboratory test before determining the theory of the formation of cusps on Roudic's beach.

In the Madsen laboratory test, as shown in Figure 22, by overlapping the edge wave and the total wave run up, it is seen that for each cycle of edge wave there is a cycle for total wave run up which is perfectly aligned. This means that in the Madsen laboratory test, the formation of coastal cusps completely follows the edge wave theory. It should be noted, however, that the reason for this exact correspondence is due to the laboratory conditions of the model, smaller dimensions and regular input wave which, naturally, is not correlated with this precision and order in real terms.

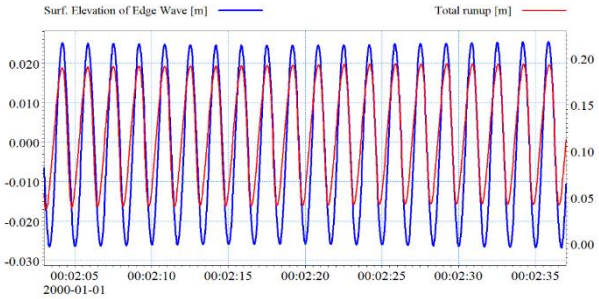

Figure 22. Total wave run up and Edge wave surface elevation in the In the Madsen laboratory test

According to above explanations, due to the actual model of the Roudic area in ocean wave scenarios, the comparison between the edge wave and the total wave run up is shown in Figure 23, part A-I, hence:

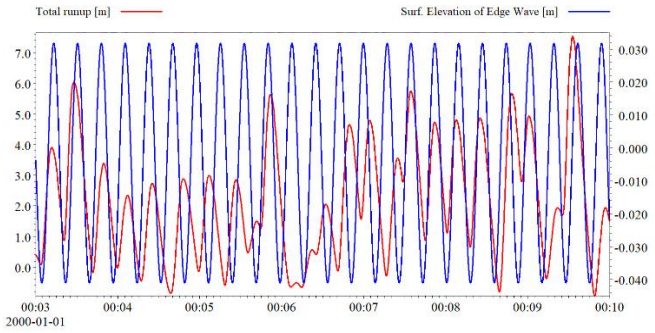

B) Scenario No. 2

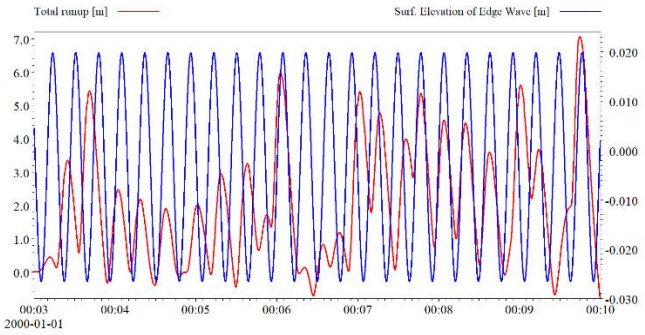

A) Scenario No. 1

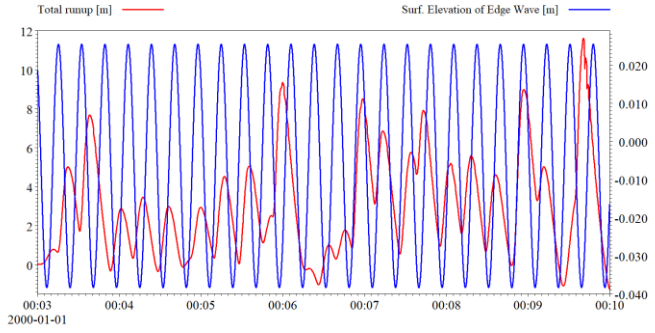

D) Scenario No. 4

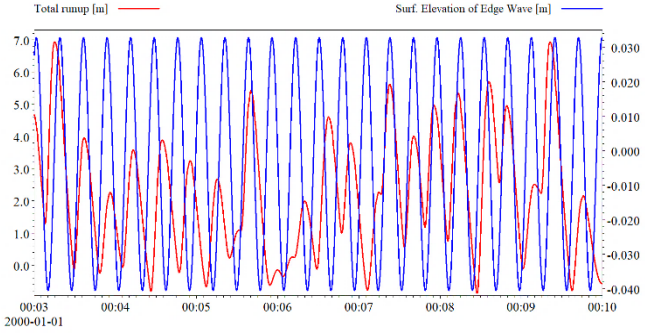

C) Scenario No. 3

[Downloaded from ijmt.ir on 2026-02-16]

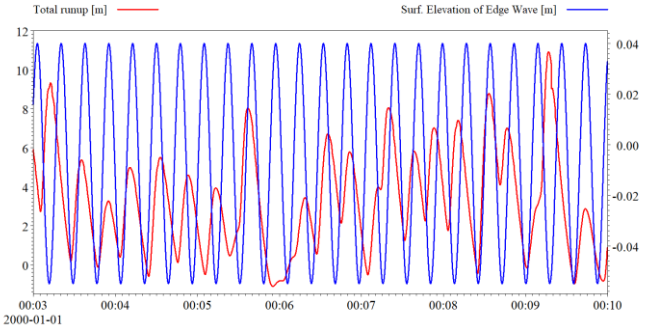

F) Scenario No. 6

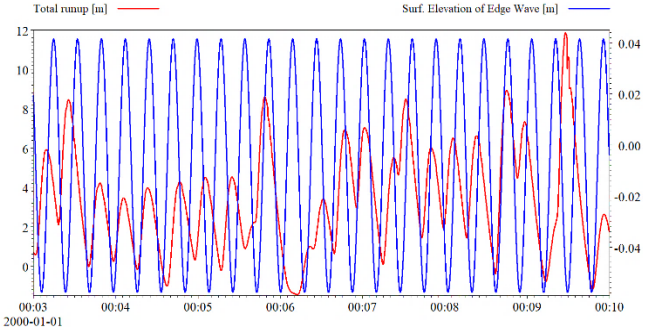

E) Scenario No. 5

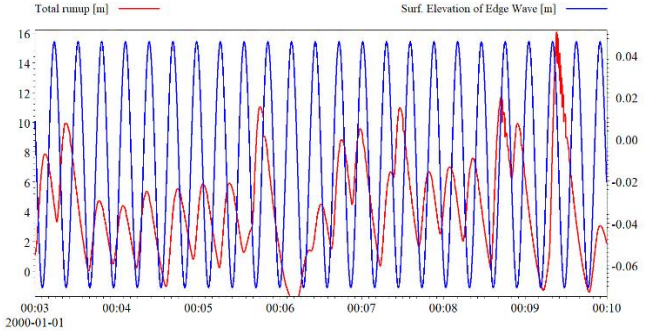

H) Scenario No. 8

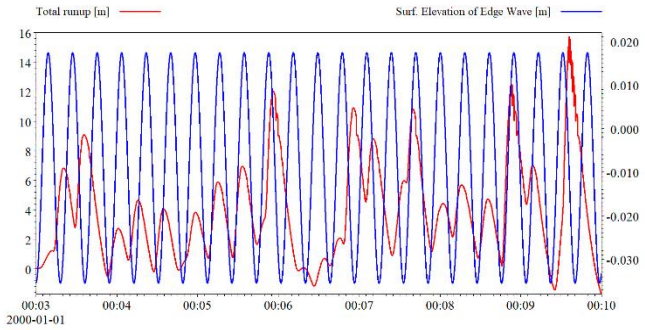

G) Scenario No. 7

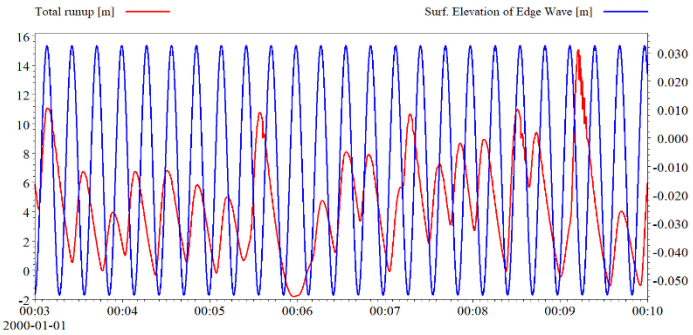

I) Scenario No. 9

Figure 23. Total wave run up and Edge wave surface elevation in the ocean wave's scenario

It can be seen that in all scenarios the alignment of the wave run up and the edge wave is relatively good. It means that for each peak in edge wave there is a summit in run up, and for each trough there is one. Of course, there is some phase difference in these shapes as compared to the experimental model, which is because of the fact that the actual conditions governing the model, such as irregular waves compare to the regular wave of the Madsen laboratory model. From this, it can be said that the beach cusps formed on the coasts of Roudic in the oceanic waves seasons are formed due to the edge wave theory. In this section, it has been proven that in the ocean wave scenarios, the edge wave theory is established. According to Table 5, the values of the intervals between the cusp's horns in the edge wave theory are more logical (according to reality), and according to Figure 16, also for the cusp of the blue line, the horn-to-horn distances between the cusps is about 7 to 11 meters.

The actual model of the coastline of the Roudic in the scenarios of the monsoon waves, according to Figure 22, sections A-I, shows the edge wave and total wave run up, hence:

[Downloaded from ijmt.ir on 2026-02-16]

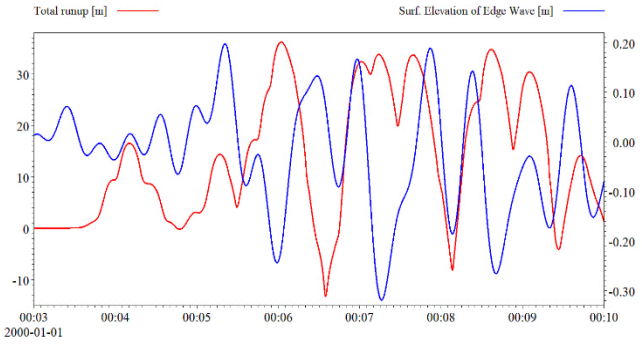

B) Scenario No. 11

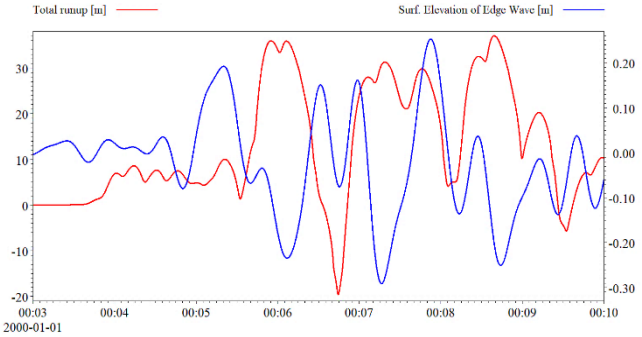

A) Scenario No. 10

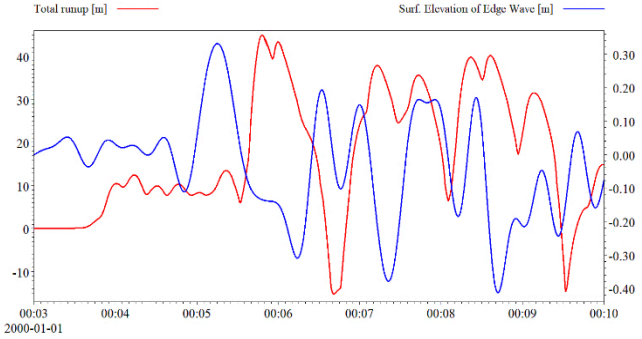

D) Scenario No. 13

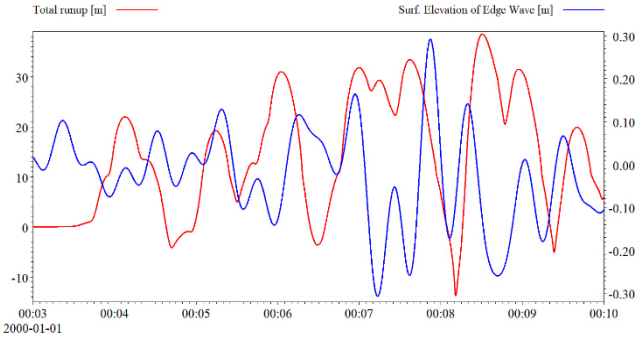

C) Scenario No. 12

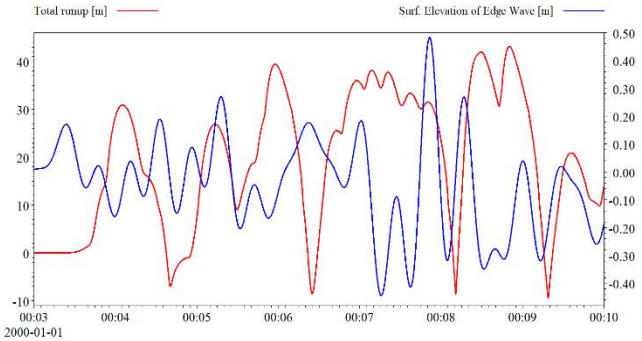

F) Scenario No. 15

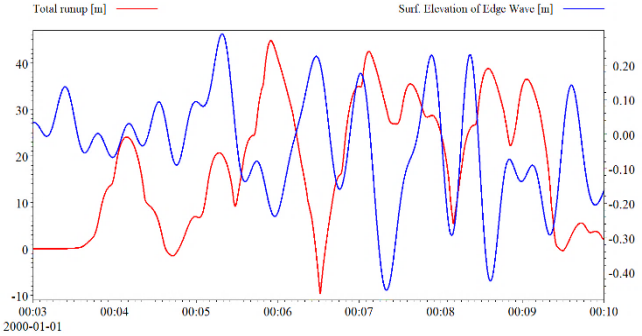

E) Scenario No. 14

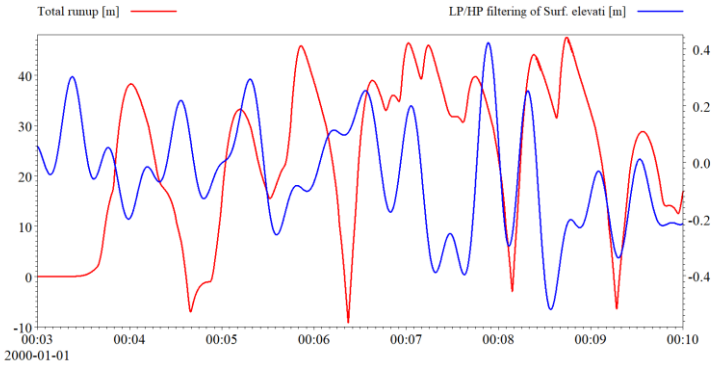

I) Scenario No. 18

Figure 24. Total wave run up and edge wave in the monsoon wave's scenario

[Downloaded from ijmt.ir on 2026-02-16]

It can be seen that in all the scenarios of monsoon waves, the alignment in the total wave run up and edge waves is not observed in any way, which means it cannot have the function of the edge wave theory. It can be said that the beach cusps formed on the coasts of the Roudic in the seasons of the Monson waves have governed by the theory of self-organization.

As shown in this section, in the scenarios of monsoon waves, the theory of self-organization is established. According to Table 6, it is observed that the values of the intervals between the cusp's horns in self-organization theory are very different from the edge wave theory, that the theory of self-organization is more rational (in accordance with reality), and due to Figure 22 for the cusps in red line, the horn-to-horn distances between the cusps is about 20 to 30 meters.

Finally, it is important to note that the EWRUC method can be used for the beaches that are relatively similar to the Roudic beach especially with a gentle slope and it can predict that the formation of beach cusps follows which theory.

7. Conclusion

Cusps change the shape of the shoreline in the short term, but under the influence of some certain conditions such as wave period, coastal gradients and wave height, their depth, distance and height will be increased or decreased and the coastline will erode. Also, if the deposition in the horns to the sea increases, it will cause sediment miss-problems for nearby structures. Therefore, knowing the status of cusp development can improve planning for projects and adopting appropriate strategies to deal with the sudden effects of coastline disruptions.

This research investigates the formation and development of Roudic's beach cusps in Chabahar in Iran. With the help of Mike 21, the effects of edge wave theory and self-organization wave theories, which has been accepted to form cusps ever since, under the influence of 18 scenarios investigated. The results of analysis of the parameters involved in the formation and modification of the cusps are presented. In this research, a new method, named by EWRUC, has been proposed, in which it is possible to determine the appropriate theory of the formation of cusps for conditions similar to the Roudic Beach. In the EWRUC method, at first, wave breaking depth was obtained in model scenarios (here Roudic coast) because the maximum energy of waves is generated in the breaking depth and edge waves are observed in this zone. The output of the surface elevation in the breaking zone is obtained by using the Mike21 software and then by using the FFT function the energy density spectrum is extracted. The maximum peak formed in the spectrum represents the edge wave. Then, taking into account the frequency range of the highest peaks generated in the edge wave energy density spectrum, the surface elevation should be extracted at that frequency range. This work was done by using the FFT function in the given interval and the extracting edge wave from it. Finally, by overlapping the extracted edge wave and the total wave run up the formation of beach cusps is determined. When the edge wave and total wave run up have the same fluctuation pattern and trend, it can certainly be noted that the beach cusps follow the edge wave theory, otherwise, cusps follow the theory of self-organization.

For the ocean waves in the Roudic area, the wave height rises from 0.5 to 1.00 meters, and the run-up ranges are 5.90 to 11.50 meters. The cusps created during oceanic waves have a horn-to-horn distance of about 7 to 11 meters. In the scenario of ocean waves, the distance between the cusps using edge wave theory, according to the distance between Roudic's beach cusps and the run up in that coastal area, confirms the edge wave theory.

In the scenario of monsoon waves in the Roudic area, the wave's height rises from 1.50 to 2.50 meters, and the run up rises from 18.80 to 35.30 meters. Cusps created during monsoon waves have a horn-to-horn distance of about 20 to 30 meters. In the scenario of monsoon waves, by considering the run up in Roudic beaches and the intervals of cusps, it can be said that the theory of self-organization is dominant.

By investigating the cusps from the edge wave theory as expressed by the EWRUC, in ocean scenarios, since there is a good coordination (in each edge wave cycle, there is a general run up cycle) between the edge wave and the total wave run up, it can be concluded that in this case the cusps follow the edge wave theory for formation. However, in monsoon scenarios, since there is no coordination between the edge wave and the total wave run up, self-organization wave theory is governing in the formation of cusps, which is consistent with the contents of the preceding paragraphs.

References

[1] Benavente J, Harris DL, Austin TP, Vila-Concejo A (2011), *Medium term behavior and evolution of a beach cusps system in a low energy beach, Port Stephens*, NSW, Australia. Journal of Coastal Research, (64), p.170

[2] Evans OF (1938) *the classification and origin of beach cusps*, The Journal of Geology, 46(4), pp.615-627.

[3] Allen JR, Psuty NR, Bauer BO, Carter RWG (1996) *A field data assessment of contemporary models of beach cusp formation*, Journal of Coastal Research, pp.622-629.

[4] Hom-ma M, Sonu C (1962) *Rhythmic pattern of longshore bars related to sediment characteristics*, Coastal Engineering Proceedings, 1(8), p.16.

[Downloaded from ijmt.ir on 2026-02-16]

[5] Sato M, Kuroki K, Shinohara T (1993) *A field experiment on the formation of beach cusps*, In Coastal Engineering 1992 (pp. 2205-2218).

[6] Coco G, Huntley DA, O'Hare TJ (2000) *Investigation of a self-organization model for beach cusp formation and development*, Journal of Geophysical Research: Oceans, 105(C9), pp.21991-22002.

[7] Masselink G, Russell P, Coco G, Huntley D (2004) *Test of edge wave forcing during formation of rhythmic beach morphology*, Journal of Geophysical Research: Oceans, 109(C6).

[8] Dodd N, Stoker AM, Calvete D, Sriariyawat A (2008) *On beach cusp formation*, Journal of Fluid Mechanics, 597, pp.145-169.

[9] Almar R, Coco G, Bryan KR, Huntley DA, Short AD, Senechal N (2008) *Video observations of beach cusp morphodynamics*, Marine geology, 254(3-4), pp.216-223.

[10] Vousdoukas MI (2012) *Erosion/accretion patterns and multiple beach cusp systems on a meso-tidal, steeply-sloping beach*, Geomorphology, 141, pp.34-46

[11] Poate TG, Masselink G, McCall RM, Russell PE, Davidson MA (2014) *Storm-driven cusp behavior on a high energy gravel beach*, Journal of Coastal Research, 70(sp1), pp.645-650.

[12] Senechal N, Laibi RA, Almar R., Castelle B, Biausque M, Lefebvre JP, Anthony EJ, Dorel M, Chuchla R, Hounkonnou MH, Penhoat YD (2014) *Observed destruction of a beach cusp system in presence of a double-coupled cusp system: the example of Grand Popo, Benin*, Journal of Coastal Research, 70(sp1), pp.669-674.

[13] Komar PD (1973) *Observations of beach cusps at Mono Lake, California*, Geological Society of America Bulletin, 84(11), pp.3593-3600.

[14] Dean RG, Maurmeyer EM (1980*) Beach cusps at point reyes and drakes bay beaches, California*, In Coastal Engineering 1980 (pp. 863-884).

[15] Inman DL, Guza RT (1982*) the origin of swash cusps on beaches*, Marine Geology, 49(1-2), pp.133-148.

[16] Masselink G, Pattiaratchi CB (1998) *Morphological evolution of beach cusps and associated swash circulation patterns*, Marine Geology, 146(1-4), pp.93-113.

[17] Williams Z (2010) *Localized Generation of Low Frequency Swash Motion through Chaotic Swash Front Interactions*, University of North Carolina Wilmington.

[18] Pruszak Z, Rozynski G, Szmytkiewicz P (2008) *Megascale rhythmic shoreline forms on a beach with multiple bars*, Oceanologia, 50(2), pp.183-203.

[19] Garnier R, Ortega-Sánchez M, Losada MA, Falqués A, Dodd N (2010) *Beach cusps and inner surf zone processes: growth or destruction? A case study of Trafalgar Beach (Cádiz, Spain)*, Scientia Marina, 74(3), pp.539-553.

[20] Birrien F, Castelle B, Dailloux D, Marieu V, Rihouey D, Price T (2013) *Video observation of megacusp evolution along a high-energy engineered sandy beach: Anglet, SW France*, Journal of Coastal Research, 65(sp2), pp.1727-1732.

[21] Otvos Jr EG (1964) *Observation of beach cusp and beach ridge formation on the Long Island Sound*, Journal of Sedimentary Research, 34(3).

[22] Holland KT (1995) *Foreshore dynamics: Swash motions and topographic interactions on natural beaches.*

[23] Sánchez M, Fachin S, Sancho F, Losada MA (2008) *Relation between beachface morphology and wave climate at Trafalgar beach (Cádiz, Spain)*, Geomorphology, 99(1-4), pp.171-185.

[24] Antia EE (1989) *Beach cusps and beach dynamics: a quantitative field appraisal*, Coastal engineering, 13(3), pp.263-272.

[25] Longuet-Higgins MS, Parkin DW (1962) *Sea waves and beach cusps*, The Geographical Journal, 128(2), pp.194-201.

[26] Idier D, Falqués A, Ruessink BG, Garnier R (2011) *Shoreline instability under low-angle wave incidence*, Journal of Geophysical Research: Earth Surface, 116(F4).

[27] Ciriano Y, Coco G, Bryan KR, Elgar S (2005) *Field observations of swash zone infragravity motions and beach cusp evolution*, Journal of Geophysical Research: Oceans, 110(C2).

[28] Guza RT, Inman DL (1975) *Edge waves and beach cusps*, Journal of Geophysical Research, 80(21), pp.2997-3012.

[29] Werner BT, Fink TM (1993) *Beach cusps as self-organized patterns*, Science, 260(5110), pp.968-971.

[30] Sriariyawat A (2010) *Formation and evolution of beach cusps, Doctoral dissertation*, University of Nottingham.

[31] Zakeri anarak E, Adjami M, Rezaei A (2017) *Numerical and analytical modeling of beach cusps formation and evolution (case study; Roudic port)*, Shahrood, Iran, MSc Thesis in Coasts ports and marine structures.

[Downloaded from ijmt.ir on 2026-02-16]

[32] Masselink G, Hegge BJ, Pattiaratchi CB (1997) *Beach cusp morphodynamics, Earth Surface Processes and Landforms*: The Journal of the British Geomorphological Group, 22(12), pp.1139-1155.

[33] Coco G, O'Hare TJ, Huntley DA (1999) *Beach cusps: a comparison of data and theories for their formation*, Journal of Coastal Research, pp.741-749.

[34] Van Gaalen JF (2011) *Alternative Statistical Methods for Analyzing Geological Phenomena: Bridging the Gap Between Scientific Disciplines*, University of South Florida.

[35] Kaneko A (1985) *Formation of beach cusps in a wave tank*, Coastal Engineering, 9(1), pp.81-98.

[36] Mangor K (2004) *Shoreline management guidelines*, DHI Water & Environment.

[37] PMO report (2017) *ICZM report*. Ministry of roads and urban development of I.R.Iran.

[38] MIKE21. BW. Manual, DHI MIKE (2014).

[39] Madsen PA, Sørensen OR, Schäffer HA (1997) *Surf zone dynamics simulated by a Boussinesq type model. Part I. Model description and cross-shore motion of regular waves*, Coastal Engineering, 32(4), pp.255-287.

[40] Mase H (1994) *Uprush-backrush interaction dominated and long wave dominated swash oscillations*, In Int. Symp. Waves-Physical and Numerical Modeling Proc. UBC, Vancouver (pp. 316-325).

[41] Nielsen AW, Simonsen HJ (2002) *Analysis of Near Field in Front of a Piston Wavemaker and MIKE 21 BW's Handling of Surfzone*, Polytechnical Midway Project, MEK, DTU.

[Downloaded from ijmt.ir on 2026-02-16]